Proceedings of the ASME 2021
International Mechanical Engineering Congress and Exposition
IMECE2021
November 1-5, 2021, Virtual, Online

IMECE2021-70454

DEVELOPMENT OF A CONTRIVED TOOL WEAR METHOD IN MACHINING

Tyler J. Grimm*
International Center
for Automotive Research
Clemson University
Greenville, SC 29607
Email: tgrimm@clemson.edu

Nils Potthoff
Virtual Machining
TU Dortmund University
Otto-Hahn-Straße 12
44227 Dortmund, Germany
Email: nils.potthoff@tu-dortmund.de

Nilesh Ashok Kharat
International Center
for Automotive Research
Clemson University
Greenville, SC 29607
Email: nkharat@clemson.edu

Laine Mears
International Center
for Automotive Research
Clemson University
Greenville, SC 29607
Email: mears@clemson.edu

Petra Wiederkehr
Virtual Machining
TU Dortmund University
Otto-Hahn-Straße 12
44227 Dortmund, Germany
Email: petra.wiederkehr@tu-dortmund.de

ABSTRACT

Tool wear in machining is generally observed as early and late stage tool wear. During early stage tool wear, the tool is rapidly worn during a break-in period, followed by a stable region of tool wear. After machining more material, the tool reaches late stage tool wear. At this point, tool wear becomes unstable; tool failure occurs quickly or it may take some time. Therefore, late stage tool wear represents a bifurcation point, making it difficult to predict tool wear past this point.

Tool wear is well known to be stochastically influenced. Due to this effect, it is difficult to perform studies on late stage tool wear since machining tools will be affected differently up to this point, introducing unknown variables. A novel method is presented in this research which utilized artificial wear to reach late stage tool wear. This method, termed contrived tool wear, may be capable of reducing the stochastic tool wear that occurs during early stage tool wear. As an initial investigation, machining tool inserts were worn by taking several passes over a grinding wheel with the tool rotating in reverse. Several parameters were tested in attempt to match the natural worn state as close as possible. Subsequent to artificial wear, the inserts were used to machine IN718. The presented method of contrived wear was found to be a good approach, but could not sufficiently replicate the tool wear typically produced in IN718 machining. Future work should aim at implementing a multi-axis approach to enable grinding at various angles to the rake face of the insert.

1 INTRODUCTION

In the energy and aerospace industry, nickel-based superalloys are often used because they meet the high requirements for strength and corrosion resistance, as well as extreme temperature resistance [1, 2]. The practical benefits of high strength and temperature resistance, however, makes machining these materials relatively difficult due to high process forces and the resulting rapid tool wear [3–5]. Especially in machining of Inconel 718 (IN718), tools have to be replaced after a very short operational time [6]. To counteract this, various studies on productivity enhancements have been investigated (e.g. alternative path strategies such as trochoidal milling [7] or the analysis of different

*Address all correspondence to this author.

cutting speeds [8]). Furthermore, investigations addressing the stochastic nature of tool wear have been conducted [9]. In addition, the influence of tool wear on process forces considering different cutting conditions and different path strategies were targeted as well [10]. However, to improve the machining of IN718, further studies necessitate to be performed which target this objective.

Tool wear studies are often characterized by the performance of a significant number of tests and the use of large volumes of materials. This must be done in order to deduce significance of results, a challenging endeavor due to the variability natural to tool wear. A common challenge faces by scientists is that in order to investigate a particular level of tool wear, the tool must first be worn to that stage. Therefore, even if only the later stages of tool wear are to be investigated, a significant amount of material must first be machined in order to produce such tool wear.

To avoid time-consuming and cost-intensive experiments for generating tool wear, inserts can be artificially worn out to a desired wear state. By controlling this process, tool wear can be accelerated and the amount of material used during testing would be reduced. Bleicher *et al.* [11] presented a method for the identification of chipping during the process, in which inserts have been worn out artificially in order to reproduce naturally occurring tool wear that has been produced through conventional machining. This process enables much more consistent tool wear results since the stochastic nature of tool wear may be decoupled in the artificial wear method.

Therefore, this paper presents a methodology for decoupling tool wear by creating artificially worn inserts. For this, the generation of artificial and natural tool wear is described in Section 2 to reproduce the typical tool wear that occurs during the machining of IN718. For fine-grained testing, skiving experiments were conducted and the inserts produced were analyzed. In Section 3, the resulting contrived and naturally worn inserts are compared and the process forces of skiving experiments are discussed. Finally, a conclusion and an outlook for future investigations are given in Section 4 and 5.

2 MATERIAL AND METHODS

For the development of a methodology for the generation of contrived wear for decoupling tool wear from the machining process, different steps are necessary. In this section, the materials and machines used are described for reference inserts with natural tool wear and for the generation of artificially worn inserts. In addition, the experimental setup for the validation – skiving experiments – is shown.

2.1 Milling tests for natural tool wear

In previous investigations, the wear development during milling of IN718 was analyzed [10]. For the investigation of different wear states, reference inserts are required which represent real wear states during milling of IN718. For this purpose, linear paths were milled on a five-axis machining center (DMG MORI DMU 50) using a CoroMill® R390-016A16-11L square shoulder milling cutter with carbide inserts (Sandvik Coromant R390-11 T3 08M-PM 1130) with multilayer AlTiCrN coating. This tool/insert combination has two flutes, a cutting diameter of d = 15.875 mm, a wiper edge length of b_s=1.2 mm, and a corner radius of r_c = 0.8 mm. A cutting speed of v_c = 40 m min^{-1}, a feed per tooth of f_z = 0.1 mm, and a width and depth of cut of $a_e = a_p$ = 1 mm were chosen, referring to [10]. The processes were conducted without cooling lubricant supply. The experimental setup is shown in Fig. 1a.

Three representative wear states – with a flank wear width of VB = 150 µm, VB = 300 µm and VB = 450 µm – were tested herein. These wear widths approximately correspond to the initial, steady state, and collapse stage tool wear, respectively. These wear states were achieved after machining the material removal equivalent of V_w = 1070 mm^3 to V_w = 2247 mm^3. In order to ensure these flank wear widths were closely achieved, it was measured iteratively between machining passes until the desired wear state was reached.

2.2 Creating artificial tool wear

In order to reproduce the previously defined conditions as closely as possible to the actual milling process, a silicon carbide (SiC) grinding wheel with a resinoid bonding was used to set up a comparable test environment on the same machining center, with the difference that the tool rotated counterclockwise (negative direction of rotation). By utilizing reversed rotation, it was ensured that the grinding wheel was not milled, but rather a slight abrasion occurred on the cutting edge. However, it was discovered after the experiments that the grinding wheel becomes consumed after contacting the tool. The test setup for producing contrived wear is shown in Fig. 1b.

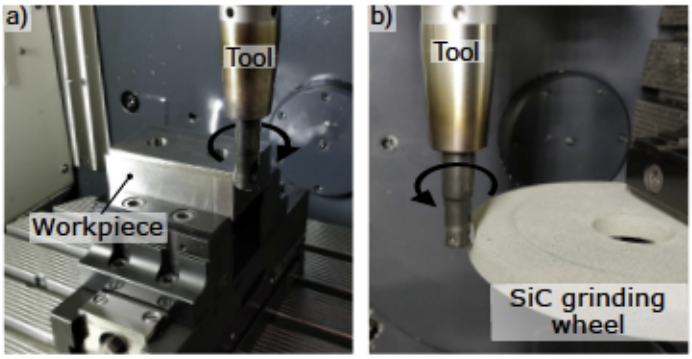

FIGURE 1. EXPERIMENTAL SETUP OF (A) THE MILLING EXPERIMENTS IN IN718 AND (B) THE ARTIFICIAL WEAR GENERATION SETUP WITH SIC GRINDING WHEEL.

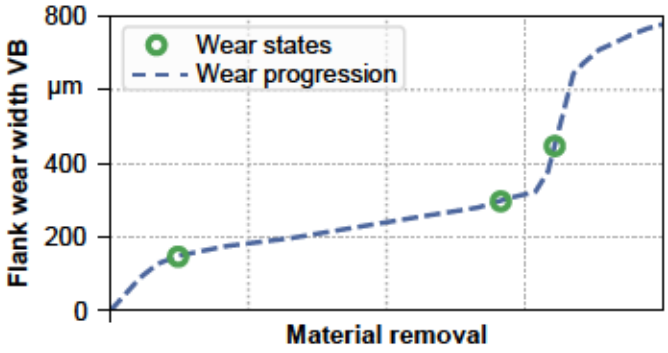

FIGURE 2. SCHEMATIC TOOL WEAR PROGRESSION (BLUE) BASED ON PREVIOUS INVESTIGATIONS WITH MARKED STATES (GREEN) – INITIAL, STEADY STATE, AND COLLAPSE STAGE BASED ON [10]

These SiC grinding wheels are commonly used for dressing grinding tools. Due to the hard abrasive material (silicon carbide) with an average grain size of 105 µm, it was hypothesized that a defined tool wear condition could be generated without the stochastic influences commonly seen in traditional tool wear. As previously stated, by decoupling tool wear from any stochastic influences, it can be repeated reproducibly.

A spindle speed of $n = 796\,\mathrm{min}^{-1}$ was chosen to generate the artificial tool wear, which corresponds to the cutting velocity previously used in the milling tests. To avoid excessive stress on the cutting edge, a reduced feed per tooth value of $f_z = 0.05$ mm was used. The depth of cut was set to $a_p = 1$ mm, which also matched the natural tool wear test condition. Linear paths were ground. For this initial study, these parameters remained the same throughout grinding. In future investigations, the effects of varying these parameters will be analyzed. It is hypothesized that adjusting these parameters could lead to the generation of different wear behaviors.

In a similar manner to traditional tool wear characterization, the tool wear produced during contrived wear experiments were associated with the volume of material removed from the grinding wheel. This value is very similar to the G ratio commonly defined in grinding processes, which is the volume of material removed divided by the volume of grinding wheel consumed [12]. However, this should not be directly compared to traditional grinding, which utilizes much smaller feed rates. For example, a surface grinder will take many passes at relatively small incremental depths in order to cut materials. With the conditions used herein, this can be imagined as taking very deep passes in surface grinding. The use of higher feeds in this process was intentional. If a much lower feed were used, only the outer regions of the tool would experience any wear. However, from preliminary investigations, it was observed that tool wear occurs slightly inward on the rake face of the tool. Therefore, it was necessary to attempt to wear these regions by increasing the feed such that the grinding material could reach deeper into the tool. The effectiveness of this approach will be discussed in section 3.

The width of cut was varied throughout the whole grinding process between 5 and 35 µm and adjusted after each grinding pass, depending on the measured flank wear width. Each grinding pass was performed over a length of $l = 3$ mm. An artificially worn insert with a flank wear width of approximately VB = 450 µm could be generated with an accumulated width of cut of 0.38 mm (cf. Fig. 3). Herewith, a dependency between each infeed/width of cut and the resulting flank wear width should be derived. This test was repeated to determine the variability in such a process, which is shown in Fig. 3.

Based on this investigation, all subsequent artificially worn inserts were conducted this way with an iterative process for the required flank wear width. The contrived inserts with a consistent wear state produced were then measured and used for skiving experiments, which will be discussed in the following sections.

2.3 Measurement of inserts

For the assessment of tool wear, the flank wear width (VB) is commonly used [6,13]. In this paper, a digital microscope was initially used to record an image of the ground and naturally worn cutting edge in which the camera was positioned approximately normal to the clearance face (*i.e.* the inserts were viewed in the radial direction). Subsequently, the flank wear width was determined by measuring the wear scar. However, this determination is often subjective, as it requires researchers to manually determine the wear edge, which is often not sharply contrasted with the rest of the tool. Therefore, further comparison is required to quantify the tool wear.

Tool wear measurements were enhanced by performing 3D comparisons between the worn inserts and an unworn insert. To perform this type of measurement, a 3D point cloud of the surface of the cutting edge was captured using a confocal microscope with focus variation (Confovis TOOLinspect, 10x magnification). This allows a multidimensional comparison of the

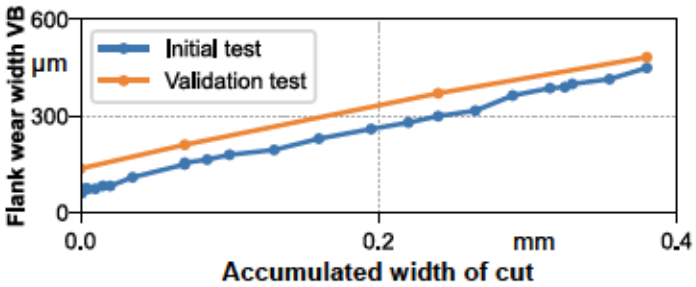

FIGURE 3. CHARACTERISTIC CURVE FOR ARTIFICIAL WEAR DEVELOPMENT OF AN INITIAL TEST AND ITS VALIDATION

affected area, which improves the quality of the assessment of the artificial wear. In Figure 4, two digitized cutting edges of a contrived insert (a) and a worn insert (b) are shown. It can be seen that natural wear has a very similar shape compared to the artificial wear. In addition, the deviation shown in Fig. 4c shows a maximum height of 30 µm which indicates a good similarity. A notable difference that can be observed in this figure is the amount of chipping that is shown in the worn insert (b) but that is not shown in the contrived insert (a). This difference between the worn and contrived inserts will be further analyzed in section 3.

2.4 Contrived insert testing

Orthogonal cutting, also known as skiving, was used to determine whether the contrived wear method utilized herein is suitable for decoupling tool wear. Herewith, an investigation of the correlation between contrived and naturally worn inserts is enabled. These validation tests were carried out on a three-axis orthogonal cutting machine tool [14], shown in Fig. 5. The utilization of such orthogonal cuts allows for a precise investigation of the occurring forces while eliminating the disturbing dynamic effects that typically occur during milling due to the high structural stiffness. Here, the tool was fixed and the feed motion was executed by the workpiece in order to perform cutting. In addition, a three-component dynamometer (Kistler 9263) was used to measure the process forces in X, Y, and Z directions, which corresponds to the force designations shown in Fig. 5 b). For comparability to the milling experiments, the surface speed of the workpiece was set to $v_f = 40\,\mathrm{m\,min^{-1}}$. This corresponded to the cutting speed during the milling experiments.

To ensure the transferability of an orthogonal cut to the milling process, the cutting conditions have to be adapted. For this purpose, the depth of cut was kept constant ($a_p = 1$ mm), but the width of cut was adapted to the feed per tooth during milling, resulting in a width of cut of $a_e = 0.1$ mm. It was possible that residual stresses induced by the tool being testing could be different between the various test conditions. In order to eliminate this variable, finishing cuts with a new insert were conducted before each test, which ensured that the material condition was the same for each test. The infeed was performed in Y direction, which corresponds to the negative normal force direction (F_n) that is shown in Fig. 5 (b).

3 RESULTS AND DISCUSSION

The contrived wear insert was compared to a naturally worn insert by analyzing the resulting surface structure of the inserts, as well as the resulting force measured in skiving experiments. In order for this contrived wear method to be effective, the results of these analyses must show significant similarities between the two wear conditions.

3.1 Analysis of flank wear width

As previously discussed, the worn tools were analyzed using microscope images and with 3D surface comparisons. Comparison images of the inserts can be seen in Fig. 6. In general, the wear shape between these tools is similar. Both tools appear worn in generally the same area. However, the surface within the worn region is different. All of the contrived wear inserts show horizontal, linear wear marks resulting from the grinding process. These types of marks are not evident in the naturally worn inserts. Instead, the surface of the naturally worn inserts are characterized by significant chipping. This can be easily seen in the wear state with a flank wear width of VB = 450 µm, shown in Fig. 6. It can be seen that the cutting edge of the naturally worn tool has a rough edge, whereas the contrived wear tool has a straight edge.

Similar results can also be observed from the 3D surface scans. For the analysis of the changed shape, the corresponding difference volume was determined. Therefore, the 3D models of the contrived and worn insert were aligned and then the difference was calculated. The resulting volume can be used as an additional measure of the quality of the grinding process. Table 1 shows the differential volume corresponding to the various wear states. In addition, the percentage deviation is shown.

The differential volumes initially indicate a very large deviation. In relation to each other, however, the percentage deviation of a contrived insert to a worn insert shows that the shapes of VB150 and VB450 deviate by approx. 31 % and 33 %, respectively. This means that about 70 % of the volume, regarding the volume of the natural worn insert, was removed by grinding the insert. The best correlation occurred with VB300, where the deviation is approx. −3.5 %, which implies that less volume was removed from the contrived insert than from the real worn insert. In addition, Fig. 7 shows the shape deviation of the 3D models of VB150 and VB450. It is hypothesized that the discrepancies between the surface of the contrived wear tool and the naturally worn tool is a result of weak bonding of the SiC particles in the grinding wheel. As the edge of the tool impacted the SiC particles, the particles were easily removed from the grinding wheel and could not exert a large force on the tool. This seems to have caused a polishing effect, rather than the conventional chipping

TABLE 1. DIFFERENCE VOLUME OF THE CONTRIVED AND WORN INSERTS WITH PERCENTAGE DEVIATION

	VB = 150 µm	VB = 300 µm	VB = 450 µm
Difference	436,758 µm³	190,741 µm³	6,067,482 µm³
Deviation	30.99 %	−3.46 %	33.34 %

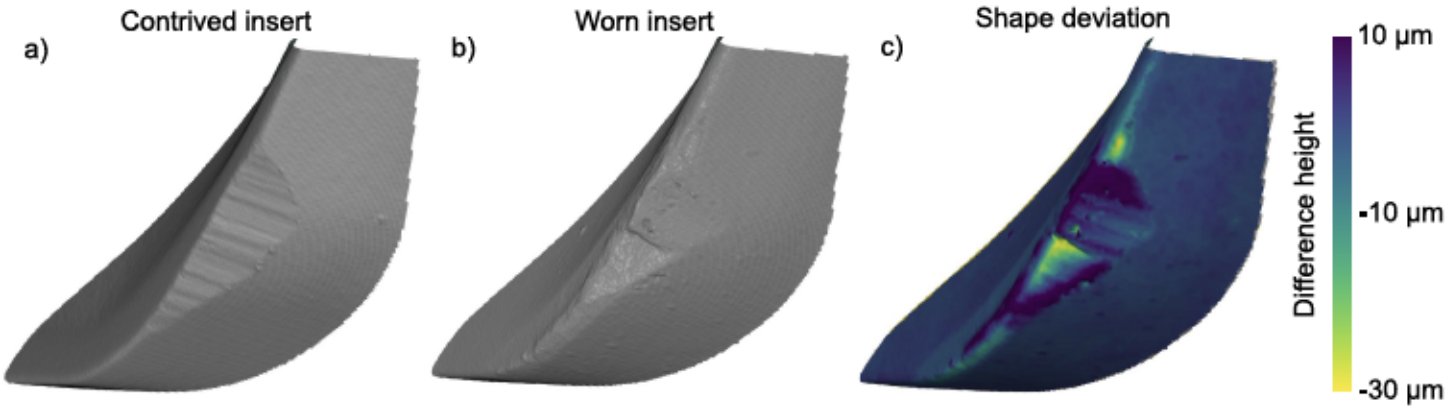

FIGURE 4. EXEMPLARY COMPARISON OF (A) A CONTRIVED INSERT WITH (B) A WORN INSERTS WITH THE SAME WIDTH OF FLANK WEAR (VB = 300 µm) AND (C) ITS DEVIATION

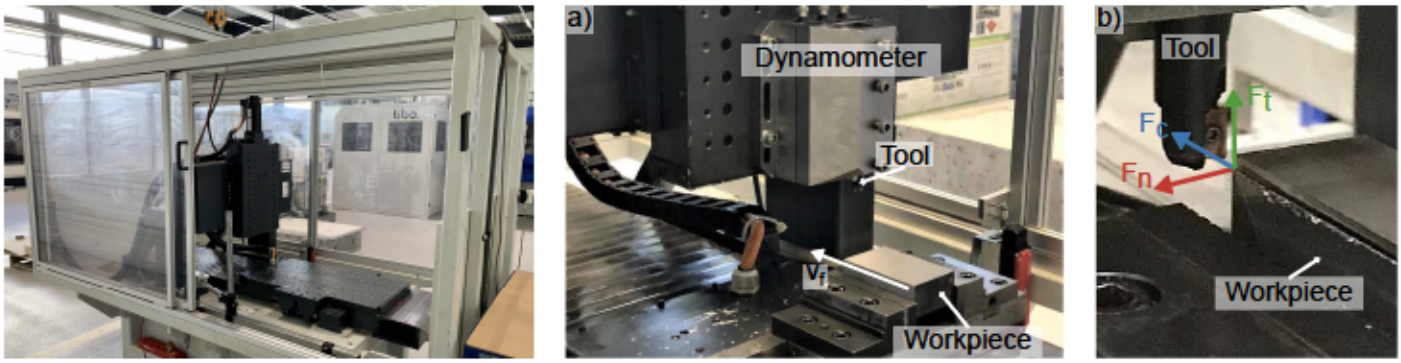

FIGURE 5. ORTHOGONAL CUTTING MACHINE WITH (A) EXPERIMENTAL SETUP OF THE SKIVING EXPERIMENTS AND (B) THE OCCURRING FORCES IN CUTTING (F_c), NORMAL (F_n), AND TANGENTIAL (F_c) DIRECTION

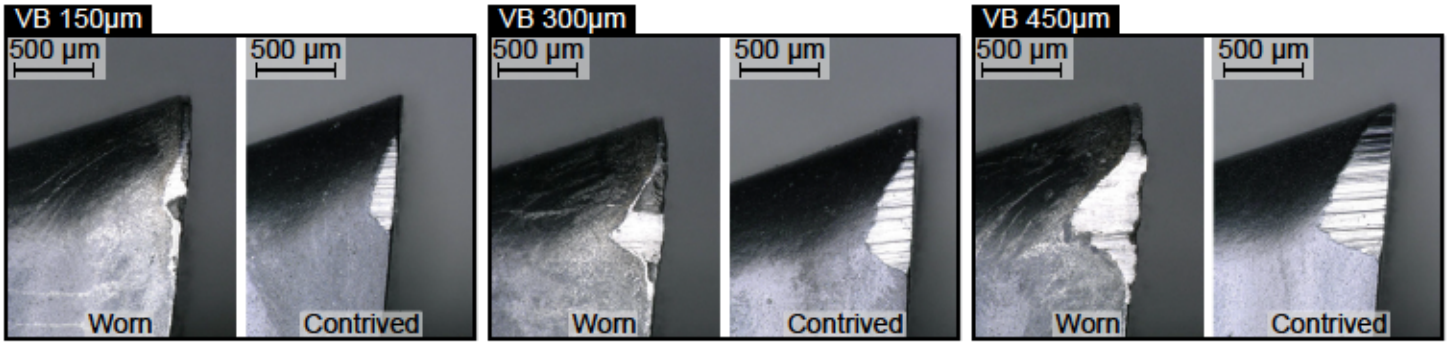

FIGURE 6. COMPARISON IMAGES OF NATURALLY AND ARTIFICIALLY WORN INSERTS

effect seen in normal tool wear at the late stage. This also would only enable wear to be produced on the radial edge of the insert. As the tool is rotating, these outer regions would contact the grinding wheel first and would not allow the interior regions of the insert to be worn by the grinding wheel. This effect is illustrated in Fig. 8.

3.2 Process forces of the skiving experiments

Based on the microscopic images and the comparisons from the 3D data, an initial evaluation of contrived and naturally worn inserts was conducted regarding their suitability for further investigations. However, in order to further validate the grinding methodology, the resulting machining forces must be investigated. Using the dynamometer described in Section 2.4, process

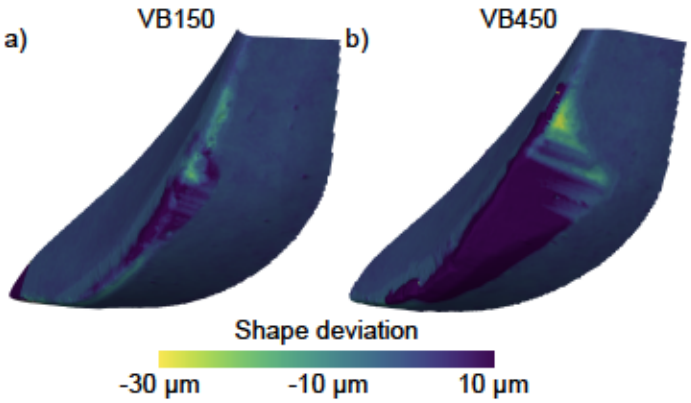

FIGURE 7. SHAPE DEVIATION OF (A) VB = 150 µm AND (B) VB = 450 µm

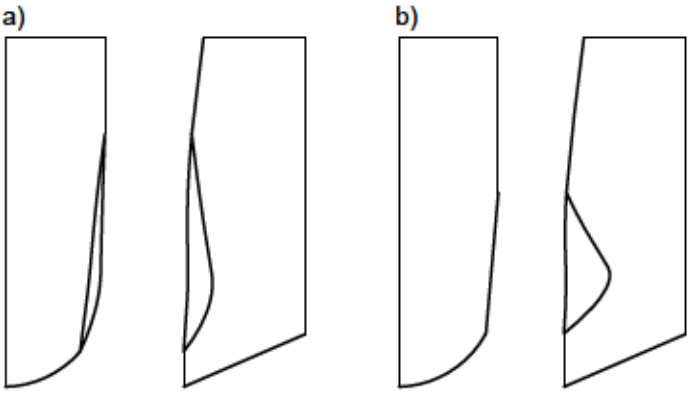

FIGURE 8. FIGURATIVE REPRESENTATION OF TOOL WEAR IN (A) NATURALLY WORN CASE AND (B) CONTRIVED WEAR CASE

forces were recorded in all three spatial directions at a sampling rate of 100,000 Hz. This sampling frequency was selected to be able to capture any of the chatter or other dynamic behaviors that may occur during testing. The process force in X direction corresponds to the normal force, in Y direction to the tangential force, and in Z direction to the cutting force (see Fig. 5).

Figure 9 shows the process forces of the contrived insert testing with a flank wear width of VB = 150 µm. In blue, the occurring process force of a new insert is shown, which serves as a reference. The process force of a naturally worn insert (green) is compared to the artificially worn insert (blue). It can be seen that higher process forces occurred with a worn insert. The effect is likely the result of several factors. For example, the undeformed chip shape can be used to explain this effect [15]. The worn cutting edge leads to a change in the contour with which the material is machined, resulting in an increase in the chip cross-sectional area. Due to the linear dependency of the chip cross-section and the process force, it will be increased. Another factor to be considered is the topology of the inserts. The naturally worn insert presents a much rougher cutting edge, as compared to the contrived wear insert which maintained a relatively sharp cutting edge.

The oscillating tangential forces can be explained by the purely lateral infeed. It is hypothesized that primarily friction and squeezing effects occurred, which lead to the strong oscillations caused by the the small volume to be machined induced by the corner radius of the cutting edge. The tangential forces were included for the sake of completeness, but do not provide a basis for analysis. In contrast, the process forces in normal direction show a very similar force level of approx. $F_n = 370\,N$ with respect to the worn and contrived insert. The comparison with the cutting force F_c, however, shows that despite the similarity of worn and contrived insert, the forces are not the same, since a difference of approx. 230 N occurs with an average force value of $F_{c,contrived} = 390\,N$ and $F_{c,worn} = 620\,N$. The significantly increased cutting force with the natural worn insert can be explained by a breakout at the cutting edge (cf. Fig. 9).

The analysis of the process forces regarding a flank wear width of VB = 300 µm in Fig. 10 shows a very good agreement of the occurring forces in normal and cutting direction. The normal forces of the worn and contrived inserts reach a force level of approx. $F_n = 470\,N$. The cutting forces ($F_c = 430\,N$) of worn and contrived inserts in relation to the reference (new) insert indicate that abrasive wear on the cutting edge primarily causes a change of the process force in normal direction, as long as the geometric shape is not changed significantly.

With a flank wear width of VB = 450 µm, the normal forces of a worn and contrived insert show a good accordance (approx. $F_n = 720\,N$) and were significantly increased compared to the reference measurement (see Fig. 11). In contrast, the cutting force shows that the natural worn insert produced a slightly increased process force compared to the reference insert, while the contrived insert exhibits a reduced force.

Due to the specific profile of the contrived insert defined by the rake face, the difference of the occurring process forces can be explained. This suggests that an adjustment of the ar-

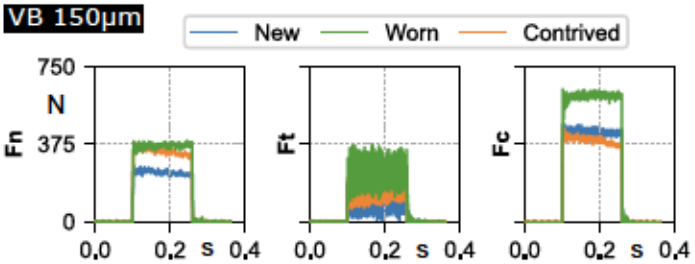

FIGURE 9. PROCESS FORCES OF A WORN AND CONTRIVED INSERT COMPARED TO A REFERENCE (NEW) INSERT OF WEAR STATE (VB = 150 µm)

tificial wear generation regarding the axial displacement of the cutting edge is essential to ensure correct decoupling. This effect is clearly visible when comparing the worn insert with the profile of the contrived insert (see Fig. 12).

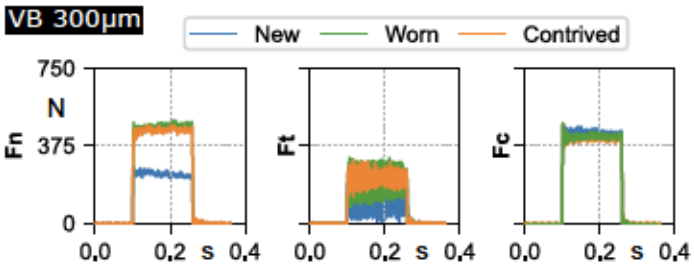

FIGURE 10. PROCESS FORCES OF A WORN AND CONTRIVED INSERT COMPARED TO A REFERENCE (NEW) INSERT OF WEAR STATE (VB = 300 µm)

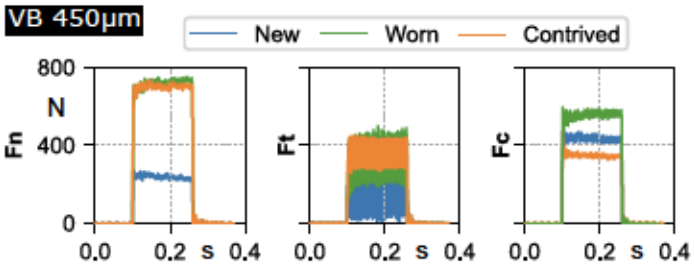

FIGURE 11. PROCESS FORCES OF A WORN AND CONTRIVED INSERT COMPARED TO A REFERENCE (NEW) (VB = 450 µm)

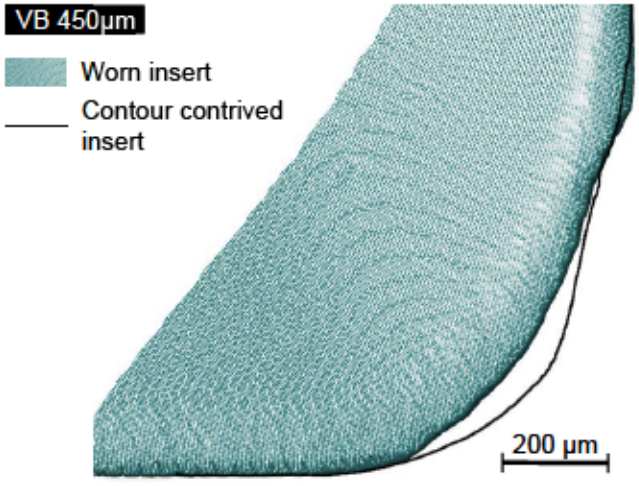

FIGURE 12. COMPARISON OF WORN INSERT WITH CONTOUR OF CONTRIVED INSERT

4 CONCLUSIONS

In order to decouple the stochastic nature of tool wear, machining inserts were artificially worn by making machining passes over a grinding wheel. Microscope images and 3D scanned surfaces were used to compare the artificially worn tools to tools which have been worn through traditional machining. The following conclusions have been made related to this work:

- the contrived wear method explored herein is capable of reproducing the general wear shape, but cannot replicate the surface structure of a naturally worn tool,
- artificially worn tools result in lower machining forces than what is observed using naturally worn tools,
- the 3D models in combination with the occurring forces showed that the shape of the contrived inserts is essential for an exact replication.

5 FUTURE WORK

As previously stated, replicating the depth of the wear using this method did not lead to the expected results. Therefore, it may be necessary to utilize a different method for artificially worn tools. The improved method proposed includes mounting the tool to the machine bed and using a relatively small grinding wheel as the rotating tool. By doing this, there will be much greater control over the positioning of the wear. An example of this can be seen in Fig. 13. This figure demonstrates that rotating the tool during the grinding process (shown in a) only allows for grinding of the outer surfaces of the insert. However, if this is reversed and the grinding wheel is rotated, the artificial wear on the cutting edge can be set to any angle. It is hypothesized that grinding the inserts at a different angle will produce results more similar to the natural wear case.

ACKNOWLEDGEMENTS

The investigations are based on the research project "Stochastic Modeling of the Interaction of Tool Wear and the Machining Affected Zone in Nickel-Based Superalloys and Application in Dynamic Stability", which is kindly funded by the German Research Foundation (DFG – 400845424) and the National Science Foundation under Grant No. 1760809. Any opinions, findings, and conclusions or recommendations expressed in this material are those of the authors and do not necessarily reflect the views of the National Science Foundation.

REFERENCES

[1] Wu BH, Zheng CY, Luo M, and He XD. Investigation of trochoidal milling nickel-based superalloy. In *Materials Science Forum*, volume 723, pages 332–336. Trans Tech Publ, 2012.

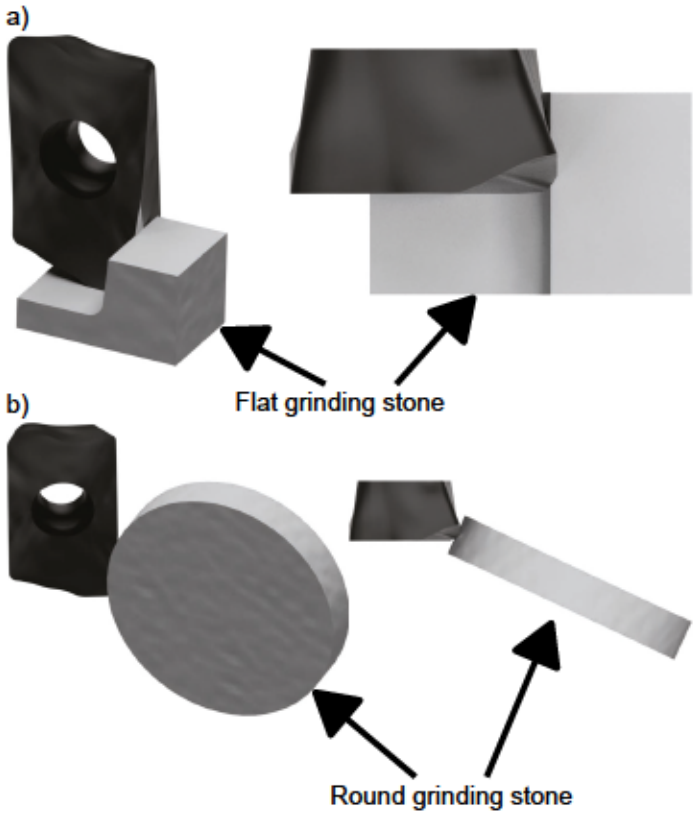

FIGURE 13. COMPARISON OF GRINDING METHODS: A) ROTATING TOOL, STATIONARY GRINDING WHEEL; B) STATIONARY TOOL, ROTATING GRINDING WHEEL

[2] Thakur A and Gangopadhyay S. State-of-the-art in surface integrity in machining of nickel-based super alloys. *International Journal of Machine Tools and Manufacture*, 100:25–54, 2016.

[3] Ulutan D and Ozel T. Machining induced surface integrity in titanium and nickel alloys: A review. *International Journal of Machine Tools and Manufacture*, 51(3):250–280, 2011.

[4] Ezugwu EO and Pashby IR. High speed milling of nickel-based superalloys. *Journal of materials processing technology*, 33(4):429–437, 1992.

[5] Ezugwu EO, Wang ZM, and Machado AR. The machinability of nickel-based alloys: a review. *Journal of Materials Processing Technology*, 86(1-3):1–16, 1999.

[6] Cantero JL, Díaz-Álvarez J, Miguélez MH, and Marín NC. Analysis of tool wear patterns in finishing turning of Inconel 718. *Wear*, 297(1-2):885–894, 2013.

[7] Pleta A, Ulutan D, and Mears L. Investigation of trochoidal milling in nickel-based superalloy Inconel 738 and comparison with end milling. In *International Manufacturing Science and Engineering Conference*, volume 45813, page V002T02A058. American Society of Mechanical Engineers, 2014.

[8] Altin A, Nalbant M, and Taskesen A. The effects of cutting speed on tool wear and tool life when machining Inconel 718 with ceramic tools. *Materials & design*, 28(9):2518–2522, 2007.

[9] Niaki FA, Ulutan D, and Mears L. Stochastic tool wear assessment in milling difficult to machine alloys. *International Journal of Mechatronics and Manufacturing Systems*, 8(3-4):134–159, 2015.

[10] Potthoff N and Wiederkehr P. Fundamental investigations on wear evolution of machining Inconel 718. *Procedia CIRP*, 99C:171–176, 2021.

[11] Bleicher F, Ramsauer CM, Oswald R, Leder N, and Schoerghofer P. Method for determining edge chipping in milling based on tool holder vibration measurements. *CIRP Annals*, 69(1):101–104, 2020.

[12] Rowe BW. 5 - wheel contact and wear effects. In W. Brian Rowe, editor, *Principles of Modern Grinding Technology (Second Edition)*, pages 83–99. William Andrew Publishing, Oxford, second edition edition, 2014.

[13] Devillez A, Le Coz G, Dominiak S, and Dudzinski D. Dry machining of Inconel 718, workpiece surface integrity. *Journal of Materials Processing Technology*, 211(10):1590–1598, 2011.

[14] Wöste F, Baumann J, Bergmann J, Garcia Carballo R, and Wiederkehr P. Experimental setup for analyzing fundamentals of cutting processes using a modular system. *Modern Machinery (MM) Science Journal*, pages 3754–3758, 2020.

[15] Pleta A, Niaki FA, and Mears L. Investigation of chip thickness and force modelling of trochoidal milling. *Procedia Manufacturing*, 10:612–621, 2017.